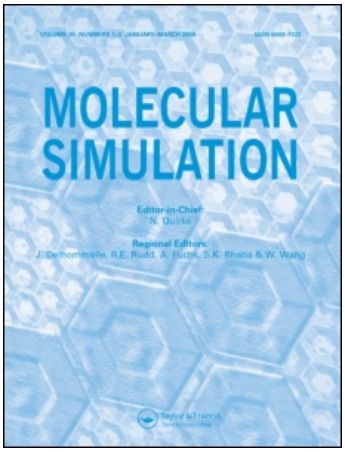

Molecular Simulation
Publication details, including instructions for authors and subscription information:
http://www.informaworld.com/smpp/title~content=t713644482

Rotational Motion of Linear Molecules in Three Dimensions. A Path-Integral Monte Carlo Approach

D. Marx[ab]
[a] Institut für Physik, Universität Mainz, Mainz, FRG [b] IBM Research Division, Zurich Research Laboratory, Rüschlikon

To cite this Article Marx, D.(1994) 'Rotational Motion of Linear Molecules in Three Dimensions. A Path-Integral Monte Carlo Approach', Molecular Simulation, 12: 1, 33 — 48
To link to this Article: DOI: 10.1080/08927029408022534
URL: http://dx.doi.org/10.1080/08927029408022534

Molecular Simulation, 1994, Vol. 12(1), pp. 33–48
Reprints available directly from the publisher
Photocopying permitted by license only

ROTATIONAL MOTION OF LINEAR MOLECULES IN THREE DIMENSIONS: A PATH-INTEGRAL MONTE CARLO APPROACH

D. MARX

Institut für Physik, Universität Mainz, Staudinger Weg 7, D-55099 Mainz, FRG

(Received January 1993, accepted June 1993)

A path-integral Monte Carlo (PIMC) simulation method for the rotational motion of linear molecules in three dimensions is presented. The technique is applied to an H_2 impurity in a static crystal-field. The resulting orientational distributions from quantum and classical simulations are obtained and discussed. The algorithm suffers from the "sign problem" of quantum simulations. However, as can be seen by comparing the low temperature simulation result to the variational solution of the Schrödinger equation, the PIMC method captures the quantum fluctuations.

KEY WORDS: Path-integral Monte Carlo simulation, rotations, linear molecules, quantum effects, sign problem

I INTRODUCTION

During the last decade, path-integral Monte Carlo (PIMC) methods [1–8] have become practical and powerful tools for studying *finite*-temperature *many*-body quantum systems starting from a microscopic description. However, most of the effort concerning continuous degrees of freedom was put in the development of PIMC methods to deal with translations, for a recent review see Reference 8. In case of *molecules*, "internal quantum states" [9–16] as e.g. rotational degrees of freedom [14–16] are relevant in addition to the translations. Rossky and coworkers [18] did include rotational motion in their PIMC treatment of water, but since they simulated at ambient temperatures they included rotations only on the quasiclassical level keeping quadratic quantum fluctuations via the van Vleck-Pauli-Morette determinant. Recently, quantum H_2 was investigated under various aspects [19, 20], but the molecule was represented in the fused-atom-approximation as a single structureless interacting site so that only the translations were quantized in these PIMC simulations. In many real systems, the molecular center of mass is confined to regular lattice sites and the molecules perform rotations in this translationally frozen-in situation [17]. Especially molecular adsorbates [21,22] as H_2 isotopes [23–29] or N_2[16,17,30–40] on graphite show registered phases with frozen-in positions of the center of mass. Only at quite low temperatures, the molecular axes order and the system undergoes a phase transition from an orientationally disordered

Present address: IBM Research Division, Zurich Research Laboratory, Säumerstr. 4, CH-8803 Rüschlikon.

high-temperature phase to the orientationally ordered behavior; the centers of mass stay in the vicinity of this phase transition at the lattice positions of the registered structure. Since such transitions of non-translational degrees of freedom occur at low temperatures, quantum fluctuations are expected to affect the transition temperature [16]. In addition, it is well established that mean-field approximations fail to predict quantitatively properties of such low-dimensional systems, as e.g. shown for a specific model adsorbate in References [9, 10].

Considering this situation, a *molecular* simulation approach [41] to non-translational degrees of freedom is desirable in the framework of *quantum* simulations. A linear rigid molecule with one rotational degree of freedom corresponds to a particle restricted to move on a circle, whereas the same molecule with two rotational axes is a particle confined to a sphere. Since the definition of the path-integral itself is strongly dependent on the manifold on which the integration is performed [42, 43], the path-integrations on the circle or on the sphere deserve special care [43]. Recently, we proposed [14, 15] a PIMC method for linear molecules confined to rotate in two dimensions (2D), i.e. for 2D rotators, which was applied to the investigation of quantum effects in a realistic interacting adsorbate of many molecules [16]. It seems that PIMC is the most promising technique for the investigation of the influence of quantum fluctuations on phase transitions occuring at non-zero temperatures [8] beyond mean-field-like approaches.

In the present paper, a first attempt is made towards the description of rotational motion of rigid linear molecules in 3D, i.e. 3D rotators, in the framework of PIMC simulations. This again requires to formulate a new version of PIMC appropriate to incorporate angular momentum operators that is quite distinct from the PIMC for 2D rotators or translational degrees of freedom. Formulation and exploration of this novel method is the aim of the present work. We describe the technique in detail and apply it to H_2 in a static crystal-field [44]. The path-integral formulation suited for PIMC simulations is introduced in Section II, the numerical techniques are presented in Section III and the application to a model is discussed in Section IV. In the last section, we summarize and give an outlook on possible future work in this direction.

II FORMULATION OF THE PATH-INTEGRAL

To describe one-particle rotational motion of rigid linear molecules, we consider in the following the standard Hamiltonian

$$\hat{H} = \frac{\hat{L}^2}{2I} + \hat{V}(\hat{\Omega}) \tag{1}$$

with the usual definitions of the angular momentum operator $\hat{L}^2|LM\rangle = \hbar^2 L(L+1)|LM\rangle$ and $\hat{\Omega}|\Omega\rangle = \Omega|\Omega\rangle$ where Ω denotes the angles (φ,ϑ); I is the moment of inertia. The potential energy V has to have the inherent symmetry of the rotator and may be chosen arbitrarily otherwise. We discretize the partition function $Z(\beta) = Tr\ \exp[-\beta\hat{H}]$ using the Trotter theorem [42, 43] in angle-space

$$Z(\beta) = \lim_{P\to\infty} \prod_{s=1}^{P} \left[\int d\,\Omega^{(s)}\right] \prod_{s=1}^{P}{}^{*}\ K_P(s, s+1)$$

$$K_P(s, s+1) = \left\langle \Omega^{(s)} \left| \exp\left[-\frac{\beta}{P} \frac{\hat{L}^2}{2I} \right] \exp\left[-\frac{\beta}{P} \hat{V}(\hat{\Omega}) \right] \right| \Omega^{(s+1)} \right\rangle, \tag{2}$$

where $K_P(s, s+1)$ denotes the high-temperature propagator matrix element. Due to the trace operation, the angular paths are closed $\Omega^{(P+1)} = \Omega^{(1)}$ as in the case of translational path-integrals which is indicated by the star. Thus, the well known "polymer language" [2,3,6] can be used: the whole path can be viewed as a ring-polymer, this time in angle-space, and the individual angles $\Omega^{(s)}$ are the "beads" of the "necklace".

At this place, a comment concerning the applicability of the Trotter decomposition in the framework of polar coordinates [45,43] should be given. In case of a general potential expressed in polar coordinates $V(r, \Omega)$, the direct discretization of the path-integral in the polar representation does not lead to the correct propagator, as is well known [43]. In this representation, the decomposition with the high-temperature propagators breaks down in the limit $r \to 0$ which occurs necessarily in the P-fold integration of the form $\int_0^\infty dr$ even in the $P \to \infty$ limit. The solution [45] is to decompose the action in cartesian coordinates and then to transform to polar coordinates. This leads [43] for radially symmetric potentials $V(r)$ to the Bessel-measure instead of the Wiener-measure for cartesian coordinates. Since we are interested in a *rigid* rotator, our potential is of the type $V(R, \Omega) = V(\Omega)$, i.e. the radial coordinate r is *fixed* to be the (bond−) length $R > 0$ of the rotator, and the Trotter decomposition can be applied without convergence problems in angle-space; together with the reduced mass μ, R is then absorbed in the moment of inertia I.

After having discussed the applicability of the Trotter decomposition in our case, the high-temperature propagators $K_P(s, s+1)$ connecting two neighboring imaginary time-slices have to be evaluated. The natural choice is to use angular momentum eigenfunctions $\Sigma_{L=0}^{\infty} \Sigma_{M=-L}^{L} |LM\rangle\langle LM| = 1$ which give as angle projections $(\Omega|LM\rangle = Y_{LM}(\Omega)$ the spherical harmonics. In this representation, the matrix elements

$$K_P(s, s+1) = \sum_{L^{(s)}=0}^{\infty} \sum_{M^{(s)}=-L^{(s)}}^{L^{(s)}} \exp\left[-\beta \left[\frac{\hbar^2 L^{(s)}(L^{(s)}+1)}{2IP} + \frac{1}{P} V(\Omega^{(s+1)}) \right] \right]$$

$$\times Y_{L^{(s)}M^{(s)}}(\Omega^{(s+1)}) \cdot Y^*_{L^{(s)}M^{(s)}}(\Omega^{(s)}) \tag{3}$$

can be further simplified using the usual addition theorem for spherical harmonics

$$\left(\frac{2L+1}{4\pi} \right) P_L(\cos \gamma^{(s,s+1)}) = \sum_{M=-L}^{L} Y_{LM}(\Omega^{(s+1)}) \cdot Y^*_{LM}(\Omega^{(s)}) \tag{4}$$

with the relative angle

$$\cos \gamma^{(s,s+1)} = \cos \vartheta^{(s+1)} \cos \vartheta^{(s)} + \sin \vartheta^{(s+1)} \sin \vartheta^{(s)} \cos(\varphi^{(s+1)} - \varphi^{(s)}) \tag{5}$$

between two time-slices. Thus after summing over the $\{M^{(s)}\}$, the K_P may be expressed as

$$K_P(s, s+1) = \sum_{L^{(s)}=0}^{\infty} \exp\left[-\beta \left[\frac{\hbar^2 L^{(s)}(L^{(s)}+1)}{2IP} \right. \right.$$

$$- \frac{1}{\beta} \ln \left[\frac{2L^{(s)} + 1}{4\pi} P_{L^{(s)}}(\cos \gamma^{(s,s+1)}) \right] + \frac{1}{P} V(\Omega^{(s+1)}) \Bigg] \Bigg], \tag{6}$$

where the Legendre polynomials are put as a "Legendre-potential" in the pseudo-Boltzmann factor. Since $-1 \leq P_L(\cos \gamma) \leq 1$ and the Legendre polynomials of degree L have as many zeros, sign and absolute value of the argument of the logarithm have to be separated

$$\ln \left[\frac{2L^{(s)} + 1}{4\pi} P_{L^{(s)}}(\cos \gamma^{(s,s+1)}) \right] = \ln \left[\frac{2L^{(s)} + 1}{4\pi} |P_{L^{(s)}}(\cos \gamma^{(s,s+1)})| \right] + i\delta(s, s+1) \tag{7}$$

introducing a phase $\exp[i\delta(s, s+1)] = \text{sign}\{P_{L^{(s)}}(\cos \gamma^{(s,s+1)})\}$ in the pseudo-Boltzmann factor. This term will give rise to the "sign problem" [46,47] as will be discussed later. Finally, the path-integral formulation of a linear molecule in an external field

$$Z(\beta) = \lim_{P \to \infty} \prod_{s=1}^{P} \left[\int d\Omega^{(s)} \sum_{L^{(s)}=0}^{\infty} \right] \exp \left[i \sum_{s=0}^{P} {}^{*} \delta(s, s+1) \right] \times \exp \left[- \beta \sum_{s=1}^{P} {}^{*} \left[\frac{\hbar^2 L^{(s)}(L^{(s)} + 1)}{2IP} - \frac{1}{\beta} \ln \left[\frac{2L^{(s)} + 1}{4\pi} |P_{L^{(s)}}(\cos \gamma^{(s,s+1)})| \right] + \frac{1}{P} V(\Omega^{(s+1)}) \right] \right] \tag{8}$$

can be written down for any suited rotational potential $V(\Omega)$.

The formulation given in (8) reduces in the free case $V(\Omega) = 0$ immediately to the partition function for the quantum mechanical linear rotator in three dimensions [48]. The term $\propto L(L+1)$ can be identified directly and the Legendre-potential gives together with the addition theorem and the P-fold integration over $\{\Omega^{(s)}\}$ only Kronecker-deltas in L and M. The classical limit, corresponding to $[\hat{L}, \hat{V}(\hat{\Omega})] = 0$, can be obtained from (8) by setting $P = 1$: the Legendre-potential becomes trivial $P_L(\cos(\gamma^{(1,1)}) = 1$, and the L-summation can be replaced by an integral.

It can be shown that expression (8) may also be derived starting from the general path-integral in polar coordinates [43]

$$Z'(\beta) = \lim_{P \to \infty} \prod_{s=1}^{P} \left[\left(\frac{2\pi\hbar^2\beta}{P\mu} \right)^{-2/3} \int_0^{\infty} dr^{(s)} r^{(s)2} \int d\Omega^{(s)} 4\pi \right] \times \prod_{s=1}^{P} {}^{*} \left[\left(\frac{\pi\hbar^2\beta}{2P\mu r^{(s)} r^{(s+1)}} \right)^{1/2} \sum_{L^{(s)}=0}^{\infty} \sum_{M^{(s)}=-L^{(s)}}^{L^{(s)}} \right.$$

$$\times\left\{I_{L^{(s)}+1/2}\left(\frac{P\mu r^{(s)}r^{(s+1)}}{\hbar^2\beta}\right) Y_{L^{(s)}M^{(s)}}(\Omega^{(s+1)})\cdot Y^*_{L^{(s)}M^{(s)}}(\Omega^{(s)})\right\}\Bigg]$$

$$\times\exp\left[-\beta\sum_{s=1}^{P}{}^{*}\left[\frac{P\mu}{2\hbar^2\beta^2}\left[r^{(s)2}+r^{(s+1)2}\right]+\frac{1}{P}\tilde{V}(r^{(s)},\Omega^{(s)})\right]\right], \quad (9)$$

if the radial coordinates $\{r^{(s)}\}$ in (9) axe fixed to R; $I_\nu(z)$ denotes the Bessel functions. Semilarly as done in Reference [49], one has to replace the full potential by the following expression

$$\exp\left[-\frac{\beta}{P}\sum_{s=1}^{P}\tilde{V}(r^{(s)},\Omega^{(s)})\right]\propto\exp\left[-\frac{\beta}{P}\sum_{s=1}^{P}V(\Omega^{(s)})\right]\prod_{s=1}^{P}\delta(r^{(s)}-R) \quad (10)$$

to enforce that the radial coordinates $\{r^{(s)}\}$ are restricted to the length R of the molecule at each time-slice. After performing the now trivial integrations $\{r^{(s)}\}$ the exact Bessel functions with fixed $R>0$

$$I_{L+1/2}\left(\frac{P\mu R^2}{\hbar^2\beta}\right)\sim\left(\frac{2\pi P\mu R^2}{\hbar^2\beta}\right)^{-1/2}\exp\left[-\beta\left[\frac{\hbar^2L(L+1)}{2P\mu R^2}-\frac{P\mu R^2}{\hbar^2\beta^2}\right]\right] \quad (11)$$

can be replaced by their asymptotic expansion [50] in the limit $P\to\infty$. However, this derivation is more cumbersome, whereas is it more natural and illustrative to start directly from the angle-dependent potential $V(\Omega)$ using the Trotter decomposition is angular space.

It is very interesting to compare the obtained representation for the 3D linear rotator with the corresponding result for the 2D case and path-integrals in cartesian coordinates [42,43]. The potential connecting two neighboring imaginary time-slices, i.e. two beads of the necklace, is much more complicated than in the other two cases. Instead of being just harmonic $\propto P\,(x^{(s)}-x^{(s+1)})^2/\beta^2$, it now consists of the logarithm of a Legendre polynomial evaluated at the relative angle $\gamma^{(s,s+1)}$ between the two angles $\Omega^{(s)}$ and $\Omega^{(s+1)}$ and additionally depends on the local L-state of the $(s,s+1)$−bond. The Legendre-potential

$$\mathscr{L}(x)=-\frac{1}{\beta}\ln\left[\frac{2L+1}{4\pi}\,|P_L(x)|\right] \quad (12)$$

diverges for $L>0$ at the zeros of the polynomials. Upon crossing such a divergence (in the MC scheme), a sign change in the integrand of the path-integral is induced by the phase $\delta(s,s+1)$, see Figure 1. These divergences in the measure of the 3D rotational path-integral find their correspondence in the nodal lines of the wave-functions in Schrödinger's representation: there exist angle configurations for which the integrand of the path-integral has to vanish. In the language of statistical mechanics, these configurations have "no weight" in (quantum-) thermal averages, i.e. such configurations will be excluded from the Markov-chain built up during a PIMC simulation. Other relative directions, where the Legendre-potential is minimal, have on the other hand a high weight. In the free case at very low temperatures, where $\{L^{(s)}=0\}$-configurations have the most weight, the relative orientations of the angles along the Trotter axis do not play a role any more and a spherically symmetric distribution along this direction arises. Being L-independent, the external potential V imposes nevertheless preferred angle directions on the rotator so that for $L^{(s)}>0$

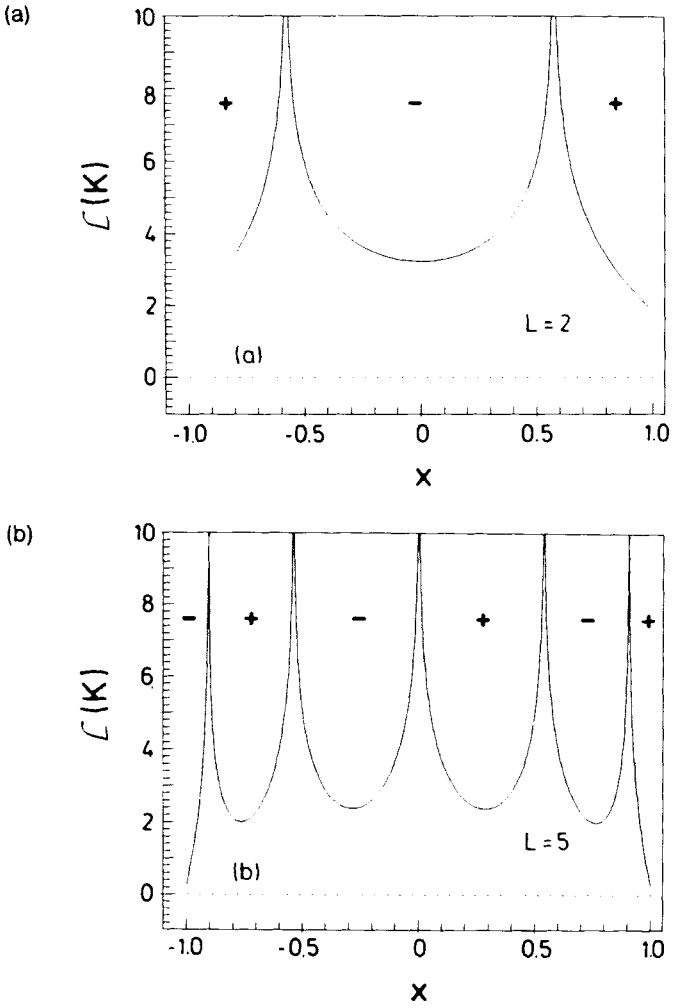

Figure 1 Legendre-potential $\mathcal{L}(x)$, see text, for $\beta = 2\,\mathrm{K}^{-1}$; where '+' and '−' mark the sign of $P_L(x)$. (a) $L = 2$. (b) $L = 5$.

aspherical angle distributions emerge due to the interplay of external potential and L-dependent Legendre-potential.

A deep difference in the concept of 2D and 3D rotational path-integrals stems from the topology of the manifold underlying the integration [42,43]. The 2D rotator is defined on the circle S^1 whereas the 3D rotator on the sphere S^2. The S^2 is a simply connected manifold, i.e. in the path-integration *all* paths (i.e. angle configurations $\{\Omega^{(s)}\}$) can be transformed into each other by purely *local* moves. For the simulation algorithm, this means that in principle (for infinitely long simulation times) only *local* changes of the dynamical variables $\{\Omega^{(s)}\}$ are sufficient to reach any point on the S^2 and as such to carry out the *complete* path-integration properly; this purely local motion is diffusive and may become unacceptably slow at low

temperatures [8], but this is a technical and not a fundamental point. It should be noted that the P discrete pseudo-quantum numbers $\{L^{(s)}\}$ are local variables in imaginary time as of course the angles themselves. With respect to the manifold, path-integrals in cartesian coordinates can also be carried out numerically using strictly local MC moves. In the framework of PIMC, 2D rotational motion is introduced only recently in Reference [14] and discussed in detail in Reference [15]. In this case, the integration manifold S^1 consists of infinitely many homotopy classes indexed by a discrete winding number $n = 0, \pm 1, \pm 2, \ldots$. Paths in two different classes cannot be transformed into each other just by local moves. Thus the winding number can be viewed as a *global* property of the whole path and in this sense, contrary to the $\{L^{(s)}\}$, as a non-local variable. As a consequence, changing the winding number of a path, i.e. changing the homotopy class, involves non-local moves in the MC-algorithm [14,15] which are in a sense similar to the moves in Worldline-MC [4] for quantum-spin systems on a lattice or permutation moves [51] in the simulation of many-boson systems. This means that one can only change the winding number of a path with also changing simultaneously the *configuration* of its variables. It should be noted explicitly that the P discrete variables $\{L^{(s)}\}$ emerging from quantum numbers in the 2D case have nothing in common with the winding number n of the 2D rotator which arises due to a Poisson-transformation [42,43,15] of the quantum number representation.

III PATH-INTEGRAL MONTE CARLO TECHNIQUE AND MODEL POTENTIAL

In order to use (8) for numerical purposes in a PIMC simulation, one has to separate sign and absolute value of the integrand [46,47]. We define averages of estimators $\langle \mathcal{O} \rangle$ introducing the positive measure

$$\begin{aligned}\langle \mathcal{O} \rangle^{(+)} = (Z^{(+)})^{-1} \cdot \lim_{P \to \infty} \prod_{s=1}^{P} \left[\int d\Omega^{(s)} \sum_{L^{(s)}=0}^{\infty} \right] \\ \times \exp\left[-\beta \sum_{s=1}^{P}{}^{*} \left[\frac{\hbar^2 L^{(s)}(L^{(s)}+1)}{2IP} \right.\right. \\ \left. - \frac{1}{\beta} \ln\left[\frac{2L^{(s)}+1}{4\pi} \left| P_{L^{(s)}}(\cos \gamma^{(s,s+1)}) \right| \right] \right. \\ \left.\left. + \frac{1}{P} V(\Omega^{(s+1)}) \right] \right] \mathcal{O}, \end{aligned} \tag{13}$$

where the partition function (8) without the phase factor $\exp[i \Sigma_{s=0}^{\infty}{}^{*} \delta(s, s+1)]$ serves now as the proper normalization $Z^{(+)}$. Using this definition, one can express the averages without any approximation as

$$\langle \mathcal{O} \rangle = \frac{\left\langle \exp\left[i \sum_{s=1}^{*P} \delta(s, s+1) \right] \mathcal{O} \right\rangle^{(+)}}{\left\langle \exp\left[i \sum_{s=1}^{*P} \delta(s, s+1) \right] \right\rangle^{(+)}}, \tag{14}$$

where the division by the mean sign of the configurations assures the correct averaging [46,47]. The sign problem [46,47] comes in case of the 3D rotators from an up to now unknown corner: it stems from the orientationally dependent Legendre-potential $\mathscr{L}$ in the pseudo-Boltzmann factor. If the relative orientation of two neighboring angles is changed in such a way that the corresponding Legendre-polynomial changes its sign, this sign change is transferred on the integrand of the path-integral.

The Legendre-potential as defined in (12) is temperature dependent, but taking into account the multiplication by β in the pseudo-Boltzmann factor, this means that this term does not contribute *explicitely* to the total energy of the rotator. Correspondingly, energy

$$\langle E \rangle = \left\langle \frac{1}{P} \sum_{s=1}^{P} [\Theta L^{(s)}(L^{(s)} + 1) + V(\Omega^{(s)})] \right\rangle \tag{15}$$

and heat capacity

$$\langle C_v \rangle = \beta^2 \{ \langle E^2 \rangle - \langle E \rangle^2 \} \tag{16}$$

do not possess any extra terms [12] which result in case of a temperature dependent effective Hamiltonian. The Legendre-potential influences only indirectly the energy via the selection of the angle configurations which are not allowed due to the divergence of this potential for $P_L(\cos \gamma) = 0$.

Similarly to the 2D algorithm [14,15], local and global moves of the angles are performed and to improve the statistics 500 independent rotators were treated in parallel. A local move consists in an attempted change of just one bead $\Omega^{(s)}$ by a random angle increment, whereas in global moves a fragment of the path $\{\Omega^{(s)} \ldots \Omega^{(s)} \ldots \Omega^{(s+f)}\}$ with random length $f = 2, , 3, \ldots P$ is chosen to be displaced. In addition to the P-fold Ω-integration on the $\mathscr{S}^2$, also the P-fold summations over the "local quantum numbers" $\{L^{(s)}\}$ have to be performed. The local quantum numbers axe tried to be changed by ± 1 only and the choice $L^{(s)} < 0$ is not allowed. In the MC loop, the type of move is selected at random, and the relative weight of 47%/6%/47% for local/global L-moves allows an efficient sampling of configurations. During one sweep over the 500 rotator system, the type of the move was the same for all rotators, but it was chosen at the beginning of each sweep at random. Together with the relative weights of the moves, this defines one MC steps.

The evaluation of the Legendre-potential needs some special attention. It is known that the Legendre-polynomials can be evaluated also for high degrees most reliably using the numerically stable [52] recursion relations [50]. But this procedure of recursively evaluating the functions would completely slow-down the algorithm for the required large L-values, if done in every MC step. We tabulated on a fine grid the Legendre-potentials defined by the first 50 Legendre-polynomials keeping also track on their sign and parity. However, for $L \geq 50$ we use an asymptotic expansion [50]

$$P_L(\cos \gamma) \sim \left(\frac{2}{\pi L \sin \gamma}\right)^{1/2} \left(1 - \frac{3}{8L}\right) \cos\left\{\left(L + \frac{1}{2}\right)\gamma - \frac{\pi}{4}\right\} \tag{17}$$

for large L and calculate the corresponding Legendre-potential directly in the simulation. Already for $L = 20$ this asymptotic L-expansion is on the scale of the variation of the function extremely accurate as compared to the exact result.

The Trotter number was $P = 240$ at 5 K and $P = 10$ at 200 K for the quantum simulations; such simulations were also performed for 20, 50, and 70 K. All simulations were started from the high temperature limit, i.e. with random orientations. Even implementing a vectorized code yielding 160 MFLOPS with $P = 240$, we needed in the low temperature quantum simulations $\approx$ 40 CPU hours for 400 000 MC steps where 40 000 MC steps were used to equilibrate the system; for the definition of our MC steps see above and all performance data are given for a CRAY-YMP. This is only a factor of not even 1.6 slower than in the 2D case: on the one hand, there are much more local degrees of freedom in the 3D rotator (two angles and one discrete variable per bead), but the time consuming "superglobal" move to sample the winding number and thus the sum over the homotopy classes of the circle is not present. The classical $P = 1$ counterpart with 1 000 000 MC steps needs only $\approx$ 0.5 hours CPU time for the 500 rotators. This corresponds to a speed per second of $\approx$ 270 000 attempted moves per rotator, whereas in the quantum case, only 1 300 attempted moves per rotator could be reached because "one quantum rotator consists of P classical rotator beads". However this is only a factor of 1/200 slower, and not 1/240 as expected from the ratio of the Trotter dimensions which has to do with the better vectorization over the "Trotter-loops" in the quantum simulations. The most serious problem of the present algorithm is the extremely severe sign problem which calls for a tremendous effort in MC steps and thus in computer time to sample sufficient statistics: 400 000 MC steps are far from being enough to establish reliable statistics.

As an application of the method, we treat an H_2 impurity in a strong static crystal-field. Such a situation in a crystal with O_h symmetry can be described using the Devonshire-potential [44]. This potential plays the role of the genuine potential for 3D rotational motion of linear molecules in a crystal as the Mathieu-potential [44] does for 2D rotational motion. The Devonshire-potential may be written as

$$V_D(\varphi, \vartheta) = -\frac{J}{8}\left[3 - 30\cos^2(\vartheta) + 35\cos^4(\vartheta) + 5\sin^4(\vartheta)\cos(4\varphi)\right] \qquad (18)$$

which is apart from a constant the lowest nontrivial cubic function [44] $K_{14}(\Omega)$ of the problem. A potential with six minima in the $\langle 100\rangle$-directions of the cubic crystal is obtained for the choice $J > 0$. The parameter $J = 10\Theta$ was chosen to model an extremely anisotropic situation; $\Theta = \hbar^2/2I = 85.3\,K$ [53] is the rotational constant of H_2. To be easily compared later on with the resulting angle distributions, the corresponding Devonshire-potential is displayed in Figure 2. This may model an anisotropic impurity as H_2 in a cubic argon matrix; a microscopic athermal treatment of the N_2 case is discussed in Reference [54] and a low temperature technique to study this problem in terms of a few-level approximation is given in Reference [55]. Comparison of the potential arising from microscopic atom-atom interactions of the impurity with the surrounding atoms in case of N_2 in Ar [54] shows that the Devonshire-potential is a very good approximation to this situation. The range between zero and extremely low temperatures of less than $\approx$ 1 K can be studied with available methods, see References [54, 55] and references therein. The crossover from extreme quantum behavior to the classical regime is not yet accessible in approaches beyond mean-field like techniques. Thus the presented PIMC formalism is the first step towards closing this methodological gap.

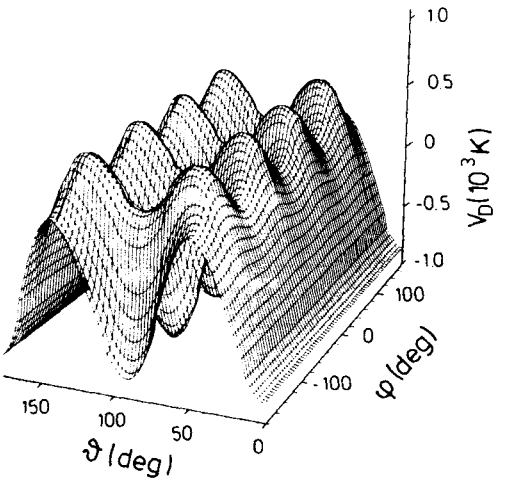

Figure 2 Devonshire-potential $V_D(\varphi, \vartheta)$ as described in the text.

IV RESULTS AND DISCUSSION

In Figure 3 and Figure 4 the angle distributions $P(\varphi, \vartheta)$ using the positive measure of an H_2 molecule in the Devonshire-potential shown in Figure 2 are displayed for low (5 K) and medium (200 K) temperatures; the quantum averages are presented in (a), and the classical treatment with all other conditions identical to the quantum simulation in (b). At 5 K in Figure 3(a) one can clearly see the impact of quantum mechanics on the angle distribution being dramatically different from the classical case in (b). Classically, the molecules are oriented with very little dispersion in the six ⟨100⟩-directions: the distribution is extremely peaked around the corresponding (φ, ϑ) combinations. The influence of the quantum fluctuations consists in "weakening the potential barriers", i.e. tunneling of the molecule allows for the population of regions which are populated classically only with vanishing probability. As a result, the quantum-mechanical angle distribution in Figure 3(a) is very smooth as compared to the classical situation in (b).

The angle distribution generated with the complete path-integral measure corresponds to the diagonal elements of the density matrix, or in the language of wave-mechanics to the thermostatistically weighted sum over the spectrum of $|\Psi_\nu(\varphi, \vartheta)|^2$ with Ψ_ν being the wavefunction corresponding to the quantum index ν. In the limit $T \to 0$ ground-state dominance is recovered and the sum over all quantum numbers collapses and gives the ground-state properties. Thus as a check of the proposed PIMC method, one can compare the angle distribution obtained by simulation at a sufficient low temperature with the exact ground-state density $|\Psi_0|^2$ from solving the Schrödinger equation. This is done in Figure 5: we show for comparison the quantity $|\Psi_0(\varphi, \vartheta)|^2$ obtained by solving numerically the Schrödinger equation of an H_2 molecule in the Devonshire-potential (18) using the Ritz-Galerkin variational method [54]. The fact that this quantity agrees quite well with the simulation result in Figure 3(a) at 5 K shows that the presented PIMC method indeed describes the

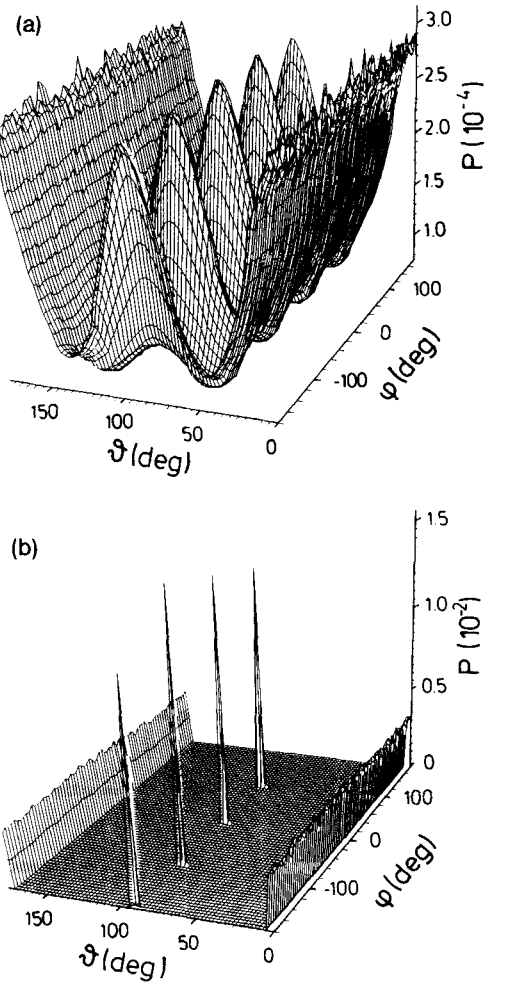

Figure 3 Angle distribution $P(\varphi, \vartheta)$ for H_2 in the Devonshire-potential, see text, at 5 K and $P = 240$. (a) Quantum averages. (b) Classical averages.

quantum nature of the rotational motion; considering the rotational constant of H_2 we expect the rotator to be for practical purposes in its ground-state at 5 K.

The rotator becomes much more classical when rising the temperature, which is visualized in Figure 4 for 200 K. The classical distribution (b) broadens because of larger thermal excitations and become qualitatively similar to the quantum result (a). But even at this temperature, one still can identify in the classical case orientations with vanishing weight. This behavior is also found [14, 15] in the strictly 2D system of H_2 adsorbed on graphite where H_2 is represented as a 2D rotator: the classical angle distribution at 5 K is dramatically different from the quantum behavior, whereas they agree qualitatively as in the present case at 200 K. The angle distributions for

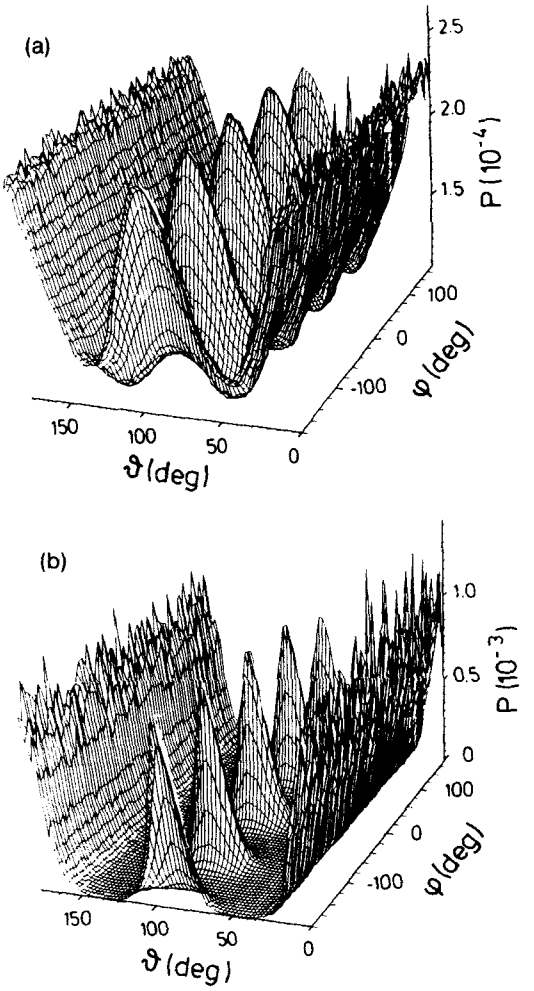

Figure 4 Angle distribution $P(\varphi, \vartheta)$ for H_2 in the Devonshire-potential, see text, at 200 K and $P = 10$. (a) Quantum averages. (b) Classical averages.

20, 50, and 70 K are qualitatively very similar to the ones shown and are therefore not presented.

With respect to the configurational properties, the proposed PIMC method produces the essential physics of quantum fluctuations and allows a direct comparison with otherwise identical classical simulations. This appealing feature of the PIMC methods allows to visualize, quantify and separate the influence of quantum effects in a given model system. However, the algorithm suffers from an extremely severe sign problem for all temperatures; in the investigated case the mean sign is typically of the order of 10^{-4}. This means that although being exact in principle, the reliable calculation of quantities as energy and heat capacity is not possible with the present

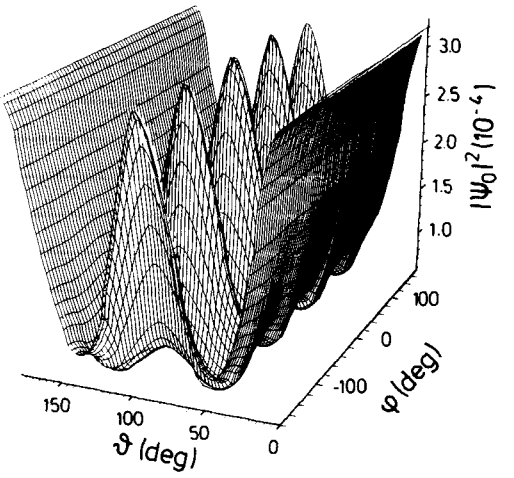

Figure 5 Square of the absolute value of the exact ground-state wavefunction $|\Psi_0(\varphi, \vartheta)|^2$ for H_2 in the Devonshire-potential, see text.

algorithm and statistics of the order of 10^6 MC steps. The reason is that the mean sign becomes very small because of the symmetric behavior of the Legendre-potential concerning sign changes, see Figure 1. The exact expression for general observables (14) exists, but statistical errors in calculating the very small mean sign call for an enormous numerical effort in order to improve the statistics. However, configurational properties as e.g. the angle distribution or derived quantities as orientational order parameters are already accessible at this stage. Since the generalization of the method for interacting many-body quantum systems is straightforward as in the 2D rotator case [15,16], the method could be used to investigate the effects of quantum fluctuations on orientational phase transitions beyond the mean-field approximation.

V CONCLUSIONS

To summarize, a numerical method based on the path-integral representation for linear molecules in three dimensions is proposed in order to investigate orientational properties of such systems in an external field. Comparing low temperature simulations, where the system is mainly in its ground-state, with variational ground-state calculations shows that the introduced path-integral Monte Carlo method produces the correct orientational distribution of a linear molecule in a static crystal-field. Thus the proposed technique is able to treat the quantum fluctuations properly and to connect smoothly quantum and classical limits with one simulation procedure. In addition, one can switch from quantum to classical simulations very easily by just changing one parameter in the program, the Trotter dimension. This has the great advantage of studying *directly* the influence of quantum effects in a particular model system.

However, the PIMC algorithm suffers severely from the well known sign problem of quantum simulations. The major drawback is that quantities like energy and heat

capacity are accessible in principle, but only with an extremely large statistical effort. The investigation of a general method to deal with highly oscillatory integrands in MC sampling, as met in real-time or many-fermion quantum simulations, is an outstanding problem of computational quantum physics. Despite impressive progress in this field such as stationary-phase [56,57] or related PIMC schemes [58,59], "analytical-fluctuation-summation-" PIMC [60], coherent-PIMC [61], "correlated"-PIMC [62], or the Maximum-Entropy approach [63], no *general* method suited for many-body PIMC simulations is known. Such a method suited also for many-rotator systems, which is the next desired step of the present approach, would help to find a better *implementation* of the presented formulation. Thus the results of this communication should be viewed *only as the first step* towards the development of a microscopic numerical method to investigate the influence of quantum fluctuations at finite temperatures on orientational phase transitions of linear molecules either on surfaces or in the bulk which goes beyond mean-field-like techniques.

Acknowledgments

It is a pleasure for me to thank P. Nielaba for his help with the Ritz-Galerkin method and K. Binder for encouraging discussions and reading the manuscript. The support (Bi 314/5 and Forschungsstipendium) from the Deutsche Forschungsgemein schaft is gratefully acknowledged, as well as grants of computer time on the Cray-YMP (Höchstleistungs-Rechenzentrum Jülich) and VP 100 (Regionales Hochschulrechenzentrum Kaiserslautern) vector processors.

References

[1] J.A. Barker, "A quantum-statistical Monte Carlo method; path integrals with boundary conditions" *J. Chem. Phys.* **70**, 2914 (1979).

[2] D. Chandler and P.G. Wolynes, "Exploiting the isomorphism between quantum theory and classical statistical mechanics of polyatomic fluids" *J. Chem. Phys.* **74**, 4078 (1981).

[3] B.J. Berne and D. Thirumalai, "On the simulation of quantum systems: path integral methods" *Ann. Rev. Phys. Chem.* **37**, 401 (1986).

[4] *Quantum Monte Carlo Methods*, M. Suzuki, ed, Springer, Berlin, 1987.

[5] *Quantum Simulations of Condensed Matter Phenomena*, J.D. Doll and J.E. Gubernatis, eds, World Scientific, Singapore, 1990.

[6] M.J. Gillan, "The path-integraal simulation of quantum systems" in *Computer Modelling of Fluids, Polymers and Solids*, C.R.A. Catlow, S.C. Parker, and M.P. Allen, eds, Kluwer, Dordrecht, 1990.

[7] D. Chandler, "Theory of quantum processes in liquids" in *Liquids, Freezing and Glass Transition*, J.P. Hansen, D. Levesque, and J. Zinn-Justin, eds, Elsevier, Amsterdam, 1991, vol. I, ch. 4.

[8] K.E. Schmidt and D.M. Ceperley, "Monte Carlo techniques for quantum fluids, solids and droplets" in *Monte Carlo Methods in Condensed Matter Physics*, K. Binder, ed, Springer, Berlin, 1992, ch. 7.

[9] D. Marx, P. Nielaba, and K. Binder, "Phase transitions in two-dimensional fluids with internal quantum states" *Phys. Rev. Lett.* **67**, 3124 (1991).

[10] D. Marx, P. Nielaba, and K. Binder, "Path-integral Monte Carlo study of a model adsorbate with internal quantum states" Phys. Rev. *B* **47**, 7788 (1993).

[11] D. Marx, "Phase diagram of a model adsorbate with internal quantum states" *Surf. Sci.* **272**, 198 (1992).

[12] D. Marx, P. Nielaba, and K. Binder, "On the calculation of the heat capacity in path-integral Monte Carlo simulations" *Int. J. Mod. Phys. C* **3**, 337 (1992).

[13] S. Sengupta, D. Marx, and P. Nielaba, "Density functional theory of magnetization driven phase transitions in fluids with internal quantum states" *Europhys. Lett.*, **20**, 383 (1992).

[14] D. Marx and P. Nielaba, "Path-integral Monte Carlo techniques for rotational motion in two

dimensions: Quenched, annealed and nospin quantum statistical averages" *Phys. Rev. A* **45**, 8968 (1992).
[15] D. Marx, S. Sengupta, and P. Nielaba, "Diatomic molecules, rotations, and path-integral Monte Carlo simulations: N_2 and H_2 on graphite" *J. Chem. Phys.* (in press).
[16] D. Marx, P. Nielaba, and K. Binder, "Quantum effects on the herringbone ordering of N_2 on graphite" Phys. Rev. Lett. **70**, 2908 (1993).
[17] S. Sengupta, O. Opitz, D. Marx, and P. Nielaba, "Herringbone orientational transition in monolayer N_2 adsorbed on graphite by density functional theory" *Europhys Lett.* (in press).
[18] G.S. Del Buono, P.J. Rossky, and J. Schnitker, "Model dependence of quantum isotope effects in liquid water" *ibid.* **95**, 3728 (1991).
[19] F.F. Abraham, J.Q. Broughton, P.W. Leung, and V. Elser, "Second-Layer Solidification of ^{3}He on Graphite: a Numerical Study" Europhys. Lett. **12**, 107 (1990).
[20] P. Sindzingre, D.M. Ceperley, and M.L. Klein, "Superfluidity in Clusters of p-H_2 Molecules" Phys. Rev. Lett. **67**, 1871 (1991).
[21] *Phase Transitions in Surface Films 2*, H. Taub, G. Torzo, H.J. Lauter, and S.C. Fain, Jr., eds, Plenum, New York, 1991.
[22] *Excitations in 2-D and 3-D Quantum Fluids*, A.F.G. Wyatt and H.J. Lauter, eds, Plenum, New York, 1991.
[23] P.R. Kubik, W.N. Hardy, and J. Glattli, "Orientational ordering of hydrogen molecules adsorbed on graphite" *Can. J. Phys.* **63**, 605 (1985).
[24] A.D. Novaco, "Phonon spectrum and density of states for the $\sqrt{3} \times \sqrt{3}R30°$ phase of D_2 and H_2 on graphite" *Phys. Rev. Lett.* **60**, 2058 (1988).
[25] A.D. Novaco and J.P. Wroblewski, "Rotational states of H_2 HD, and D_2 on graphite" *Phys. Rev. B* **39**, 11364 (1989).
[26] J.M Gottlieb and L.W. Bruch, "Uniaxial incommensurate lattice of a quantum monolayer solid" *Phys. Rev. B* **40**, 148 (1989).
[27] J.M Gottlieb and L.W. Bruch, "Calculated properties of the commensurate monolayers of helium and hydrogen on graphite" *Phys. Rev. B* **41**, 7195 (1990).
[28] W.B.J.M. Janssen, T.H.M. van den Berg, and A. van der Avoird, "Phonons and rotons in commensurate p-H_2 and o-D_2 monolayers on graphite" *Phys. Rev. B* **43**, 5329 (1991).
[29] W.B.J.M. Janssen, T.H.M. van den Berg, and A. van der Avoird, "Structure and lattice dynamics of o-H_2 and p-D_2 monolayers on graphite" *Surf. Sci.* (in press).
[30] M.H.W. Chan, A.D. Migone, K.D. Miner, and Z.R. Li, "Thermodynamic study of phase transitions of monolayer N_2 on graphite" *Phys. Rev. B* **30**, 2681 (1984).
[31] S.F. O'Shea and M.L. Klein, "Orientational phases of classical quadrupoles on a triangular net" *Chem. Phys. Lett.* **66**, 381 (1979).
[32] O.G. Mouritsen and A.J. Berlinsky, "Fluctuation-induced first-order transition in an anisotropic planar model of N_2 on graphite" *Phys. Rev. Lett.* **48**, 181 (1982).
[33] J. Talbot, D.J. Tildesley, and W.A. Steele, "A molecular dynamics simulation of nitrogen adsorbed on graphite" *Mol. Phys.* **51**, 1331 (1984).
[34] H. Evans, D.J. Tildesley, and T.J. Sluckin, "Boundary effects in the orientational ordering of adsorbed nitrogen" *J. Phys. C: Solid State Phys.* **17**, 4907 (1984).
[35] C. Peters and M.L. Klein, "Monte Carlo calculations for solid CO and N_2 overlayers physisorbed on graphite" *Mol. Phys.* **54**, 895 (1985).
[36] J. Talbot, D.J. Tildesley, and W.A. Steele, "A molecular dynamics simulation of the uniaxial phase of N_2 adsorbed on graphite" *Surf. Sci.* **169**, 71 (1986).
[37] M.P. Allen and S.F.O' Shea, "A Monte Carlo simulation study of orientational domain clusters in the planar quadrupole model" *Mol. Sim.* **1**, 47 (1987).
[38] S.E. Roosevelt and L.W. Bruch, "Lattice dynamics of thin layers of molecular nitrogen adsorbed on graphite" *Phys. Rev. B* **41**, 12236 (1990).
[39] M. Roth and R.D. Etters, "Melting transition and properties of the plastic crystal and fluid phases of N_2 deposited on graphite" *Phys. Rev. B* **44**, 6581 (1991).
[40] T.H.M. van den Berg and A. van der Avoird, "Phonons and librons in nitrogen monolayers adsorbed on graphite" *Phys. Rev. B* **43**, 13926 (1991).
[41] M.P Allen and D.J. Tildesley, *Computer simulation of liquids*, Oxford University Press, Oxford, 1987.
[42] L.S. Schulman, *Techniques and Applications of Path Integration*, Wiley, New York, 1981.
[43] H. Kleinert, *Path Integrals in Quantum Mechanics, Statistics and Polymer Physics*, World Scientific, Singapore, 1990.

[44] W. Press, *Single-Particle Rotations in Molecular Crystals*, Springer, Berlin, 1981.
[45] S.F. Edwards and Y.V. Gulyaev, "Path integrals in polar co-ordinates" *Proc. Roy. Soc. (London) A* **279**, 229 (1964).
[46] S. Sorella, S. Baroni, R. Car, and M. Parrinello, "A novel technique for the simulation of interacting fermion systems" *Europhys. Lett.* **8**, 663 (1989).
[47] E.Y. Loh Jr., J.E. Gubernatis, R.T. Scalettar, S.R. White, D.J. Scalapino, and R.L. Sugar, "Sign problem in the numerical simulation of many-electron systems" *Phys. Rev. B* **41**, 9301 (1990).
[48] D.A. McQuarrie, *Statistical Mechanics*, Harper & Row, New York, 1976.
[49] D. Peak and A. Inomata, "Summation over Feynman histories in polar coordinates" *J. Math. Phys.* **10**, 1422 (1969).
[50] Z.X. Wang and D.R. Guo, *Special Functions*, World Scientific, Singapore 1989.
[51] D.M. Ceperley and E.L. Pollock, "Path-integral computation of the low-temperature properties of liquid ^{4}He" *Phys. Rev. Lett.* **56**, 351 (1986).
[52] W.H. Press, B.P. Flannery, S.A. Teukolsky, and W.T. Vetterling, *Numerical Recipes*, Cambridge University Press, Cambridge, 1986.
[53] C.G. Gray and K.E. Gubbins *Theory of Molecular Fluids* Vol. 1, Clarendon, Oxford, 1984.
[54] P. Nielaba and K. Binder, "Lattice deformations in a N_2-Ar mixture model in the diluted limit" *Europhys. Lett.* **13**, 327 (1990).
[55] W. Helbing, P. Nielaba, and K. Binder, "Quantum Monte Carlo treatment of a rotator impurity in a crystal" *Phys. Rev. B* **44**, 4200 (1991).
[56] J.D. Doll, T.L. Beck, and D.L. Freeman, "Quantum Monte Carlo dynamics: The stationary phase Monte Carlo path integral calculation of finite temperature time correlation functions" *J. Chem. Phys.* **89**, 5753 (1988).
[57] T.L. Beck, J.D. Doll, and D.L. Freeman, "Locating stationary paths in functional integrals: An optimization method utilizing the stationary phase Monte Carlo sampling function" *J. Chem. Phys.* **90**. 3181 (1989).
[58] C.H. Mak and D. Chandler, "Solving the sign problem in quantum Monte Carlo dynamics" *Phys. Rev. A* **41**, 5709 (1990).
[59] C.H. Mak and D. Chandler, "Coherent-incoherent transition and relaxation in condensed-phase tunneling systems" *Phys. Rev. A* **44**, 2352 (1991).
[60] C.H. Mak, "Stochastic method for real-time path integrations" *Phys. Rev. Lett.* **68**, 899 (1992).
[60] T.L. Marchioro, II and T.L. Beck, "Monte Carlo evaluation of real time coherent state path integrals" *J. Chem. Phys.* **96**, 2966 (1992).
[62] W.H. Newman and A. Kuki, "Improved methods for path integral Monte Carlo integration in fermionic systems" *J. Chem. Phys.* **96**, 1409 (1992).
[63] J.E. Gubernatis, M. Jarrell, R.N. Silver, and D.S. Sivia, "Quantum Monte Carlo simulations and maximum entropy: Dynamics from imaginary-time data" *Phys. Rev. B* **44**, 6011 (1991).

Note:

Recent independent work on molecular orientational ordering was recently published by K.J. Runge, M.P. Surh, C. Mailhiot, and E.L. Pollock, *Phys. Rev. Lett.* **69**, 3527 (1992).